Organic Process Research & Development **2009**, *13*, 494–500

An Investigation of the Transformation of Carbamazepine from Anhydrate to Hydrate Using in Situ FBRM and PVM

Wenju Liu,[†] Hongyuan Wei,*[,†] and Simon Black[‡]

School of Chemical Engineering and Technology, Tianjin University, Tianjin 300072, People's Republic of China, and Process Research and Development, AstraZeneca, Macclesfield SK10 2NA, U.K.

Abstract:

This study investigated the conversion of carbamazepine (CBZ) from polymorph III to carbamazepine dihydrate (CBZH) using the in situ FBRM and PVM. The effects of agitation rate, temperature, the initial crystal size, solvent composition, and seeds were systematically studied. The transient concentration of CBZ in the solution was examined by ultraviolet spectrophotometer at the same that the solid-phase composition was quantified by offline PXRD, and the rate-controlling step for the transformation was identified. The results show that increase of agitation speed can accelerate the transformation of CBZ from polymorph III to CBZH; higher temperature or larger size of initial crystals elongated transformation time of III to CBZH greatly; seeding shortened the transformation time and the addition of ethanol-induced nucleation and accelerated the transformation.

Introduction

Polymorphism is a phenomenon related to the crystalline solid state.[1] It occurs when a molecule packs in different ways, giving rise to two or more crystal structures. Polymorphism is problematic for many industries involved in the production, development, and processing of organic solids and has attracted a lot of attention.

The transformations between anhydrous and hydrated forms in water are very similar to polymorphic transformations. It is vital to understand and control the anhydrate−hydrate phase transformation of pharmaceutical compounds. Solution-mediated transformation occurs in the presence of a solvent and is usually driven by the difference in solubility between the two forms. Solution-mediated transformations obey Ostwald's Law and involve three essential processes: (a) dissolution of the metastable solid, (b) self-recognition of the molecular units to nucleate a more stable solid phase, and (c) growth of the stable phase.

Different offline analytical techniques, namely X-ray powder diffraction (XRPD), differential scanning calorimetry (DSC), and thermal gravimetric analysis (TGA) have been used to study polymorphic transformation. Recently, a significant amount of work has been published that apply modern process analytical technology (PAT) tools[2−15] and model-based design approaches for the study of the polymorphic crystallizations. Martin Wijaya Hermanto[2] evaluates and compares the performance of the T-control, robust T-control, and C-control strategies for the polymorphic transformation of L-glutamic acid. Zoltan K. Nagy[3] uses a combination of simulations and experiments to study the comparative performance of concentration- and temperature-controlled batch crystallizations. The in situ ATR-FTIR Spectroscopy,[9] FT-Raman spectroscopy,[6,8] Raman spectroscopy,[7,10] FBRM and PVM[11,12] have been used in many studies. Review articles by Gilles Févotte, about the use of in situ infrared spectroscopy and Raman spectroscopy in pharmaceutical crystallization processes, have been published.[13,14]

Focused beam reflectance measurement (FBRM) and particle vision measurement (PVM) instruments are powerful tools developed by Lasentec as an in situ particle monitoring technique for inline real-time measurement of particle size and morphology. By measuring the change in the crystal size distribution, morphology over time, the mechanism of transformation could be identified.

Carbamazepine (CBZ) (Figure 1) is an anticonvulsant drug and exhibits four anhydrous polymorphs, a dihydrate, and a lengthy list of solvates. As a typical polymorphic compound, CBZ has been widely studied. Several authors have investigated its anhydrous polymorphs and its hydrate form.[16−33]

* Corresponding author. Telephone: +86-22-27405754. Fax: +86-22-27400287. E-mail: wenjuliu@tju.edu.cn.

[†] Tianjin University.

[‡] AstraZeneca.

(1) McCrone, W. C. *Physics and Chemistry of the Solid State*; Wiley: New York, 1965; Vol. II.

(2) Hermanto, M. W.; Chiu, Min-Sen; Woo, Xing-Yi; Braatz, R. D. *AIChE J.* **2007**, *53*, 2643–2650.

(3) Nagy, Z. K.; Chew, J. W.; Fujiwara, M.; Braatz, R. D. *Journal of Process Control* **2008**, *18*, 399–407.

(4) Braatz, R. D. *Annu.Rev. Contr.* **2002**, *26*, 87–99.

(5) Yu, L. X.; Lionberger, R. A.; Raw, A. S.; Costa, R. D.; Wu, H. Q.; Hussain, A. S. *Adv. Drug Deliver. Rev.* **2004**, *56*, 349–369.

(6) O'Brien, L. E.; Timmins, P.; Williams, A. C.; York, P. *J. Pharm. Biol. Anal.* **2004**, *36*, 335–340.

(7) Ono, T.; ter Horst, J. H.; Jansens, P. J. *Crystal Growth & Design* **2004**, *43*, 465–469.

(8) Schöll, J.; Bonalumi, D.; Vicum, L.; Müller, M.; Mazzotti, M. *Crystal Growth & Design* **2006**, *6*, 881–891.

(9) O'Sullivan, B.; Glennon, B. *Org. Process Res. Dev.* **2005**, *9*, 884–889.

(10) Giulietti, M.; Guardani, R.; Nascimento, C. A. O.; Amtz, B. *Chem. Eng. Technol.* **2003**, *26*, 267–272.

(11) Wang, Z. Z.; Wang, J. K.; Dang, L. P. *Ind. Eng. Chem. Res.* **2007**, *46*, 1851–1858.

(12) Wang, Z. Z.; Wang, J. K.; Dang, L. P. *Org. Process Res. Dev.* **2006**, *10*, 450–456.

(13) Févotte, G. *Int. J. Pharm.* **2002**, *241*, 263–278.

(14) Févotte, G. *Trans IChemE, Part A, Chemical Engineering Research and Design* **2007**, *85* (A7), 906–920.

(15) Yu, Z. Q.; Chew, J. W.; Chow, P. S.; Tan, R. B. H. *Trans IChemE, Part A, Chemical Engineering Research and Design* **2007**, *85* (A7), 893–905.

(16) Lowes, M. M. J.; Caira, M. R.; Lotter, A. P.; Van Der Watt, J. G. *J. Pharm. Sci.* **1987**, *76*, 744–752.

10.1021/op8002773 CCC: $40.75
Published on Web 02/19/2009

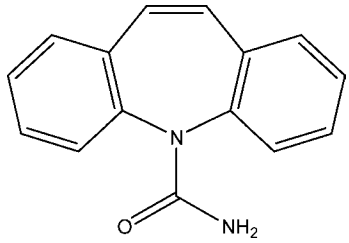

Figure 1. **Chemical structure of CBZ.**

Carbamazepine is also known to readily form a crystalline dihydrate phase of the anhydrous forms on contact with bulk water, and the transformation has been studied several times. F. Tian[34] characterized the conversion kinetics of carbamazepine polymorphs to the dihydrate in aqueous suspension using Raman spectroscopy. Haiyan Qu[35] studied the additive effects on the anhydrate−hydrate phase transformation. D. Murphy[36] investigated the effect of lattice disorder. R. Nair[37] researched the influence of polyethylene glycol and povidone on the polymorphic transformation and solubility of carbamazepine.

The morphologies of the two forms of carbamazepine are very different: CBZ polymoph III forms blocks, whereas CBZH forms thin needles.[38] In this study the in situ techniques of Lasentec PVM and FBRM were used to measure the kinetics of the transformation of CBZ form III to CBZH. Supplementary experiments were carried out using three offline techniques: powder X-ray diffraction and optical microscopy of solid samples, and UV spectroscopy of solution samples. The influences of agitation rate, temperature, crystal size, solvent composition, and seeds were studied systematically.

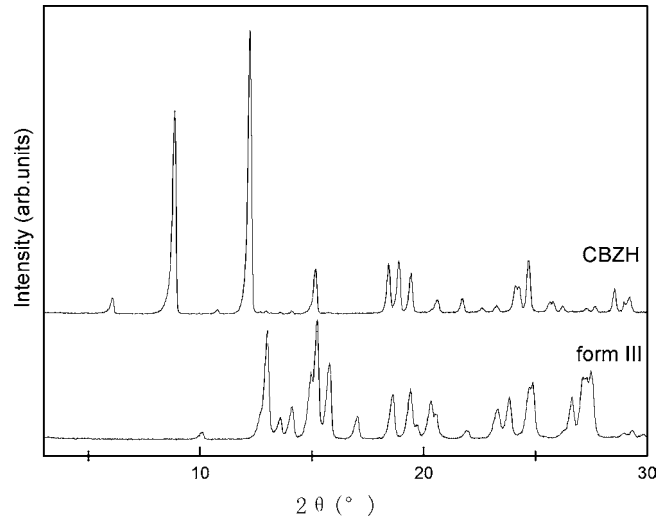

Figure 2. **XRD spectra of CBZ form III and CBZH.**

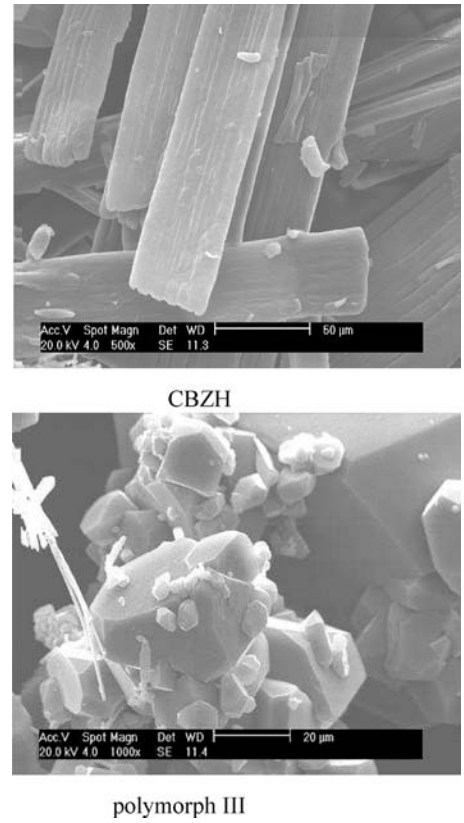

Figure 3. **SEM photographs of CBZH and CBZ form III.**

Experimental Section

Carbamazepine (CBZ), its polymorph determined by XRD, is form III and was obtained from Suzhou Hengyi Pharmaceutical Co. Ltd., China. Its purity is more than 99% (information from supplier). The ethanol (purchased from Tianjin Kewei Chemical Reagent Co., China) used for experiments was of analytical reagent grade and without any treatment before use. Distilled, deionized water was used. For both polymorphs, Figures 2 and 3 show the characteristic XRD patterns and scanning electron micrographs, respectively. It is worth noting

(17) Rustichelli, C.; Gamberini, G.; Ferioli, V.; Gamberini, M. C.; Ficarra, R.; Tommasini, S. *J. Pharm. Biol. Anal.* **2000**, *23*, 41–54.
(18) Matsuda, Y.; Akasawa, R.; Teraoka, R.; Otsuka, M. *J. Pharm.Pharmacol.* **1994**, *46*, 162–167.
(19) Krahn, F. U.; Mielck, J. B. *Pharm.Acta Helv.* **1987**, *62*, 247–254.
(20) Day, G. M.; Zeitler, J. A.; Jones, W.; Rades, T.; Taday, P. F. *J. Phys. Chem. B* **2006**, *110*, 447–456.
(21) Cabeza, A. J. C.; Day, G. M.; Samuel Motherwell, W. D.; William, J. *Crystal Growth & Design* **2006**, *6*, 1858–1866.
(22) Behme, R. J.; Brooke, D. *J. Pharm. Sci.* **1991**, *80*, 986–990.
(23) Francesca, P. A.; Fabbiani; Byrne, L. T.; McKinnon, J. J.; Spackman, M. A. *CrystEngComm* **2007**, *9*, 728–731.
(24) Grzesiak, A. L.; Lang, M.; Kim, K.; Matzger, A. J. *J. Pharm. Sci.* **2003**, *92*, 2260–2271.
(25) Gu, C. H.; Young, J.; Victor & Grant, D. J. W. *J. Pharm. Sci.* **2001**, *90*, 1878–1889.
(26) Getsoian, A.; Lodaya, R. M.; Blackburn, A. C. *Int. J. Pharm.* **2008**, *348*, 3–9.
(27) Roberts, R. J.; Payne, R. S.; Rowe, R. C. *J. Pharm. Sci.* **2000**, *9*, 277–283.
(28) Phadnis, N. V.; Cavatur, R. K.; Suryanarayanan, R. *J. Pharm. Biol. Anal.* **1997**, *15*, 929–943.
(29) Tian, F.; Zhang, F.; Sandler, N.; Gordon, K. C.; McGoverin, C. M.; Strachan, C. J. *European Journal of Pharmaceutics and Biopharmaceutics* **2007**, *66*, 466–474.
(30) Kobayashi, Y.; Ito, S.; Itai, S.; Yamamoto, K. *Journal of Pharmaceutics.* **2000**, *193*, 137–146.
(31) Gosselin, P. M.; Thibert, R.; Preda, M.; McMullena, J. N. *Int. J. Pharm.* **2003**, *252*, 225–233.
(32) AueraM., E.; Griessera, U. J.; Sawatzkib, J. *J. Mol. Struct.* **2003**, *661*−*662*, 307–317.
(33) Bettini, R.; Bonassi, L.; Castoro, V.; Rossi, A.; Zema, L.; Gazzanigab, A.; Giordanoa, F. *European Journal of Pharmaceutical Sciences* **2001**, *13*, 281–286.
(34) Tian, F.; Zeitler, J. A.; Strachan, C. J.; Saville, D. J.; Gordon, K. C.; Rades, T. *J. Pharm. Biol. Anal.* **2006**, *40*, 271–280.
(35) Qu, H. Y.; Louhi-Kultanen, M.; Kallas, J. *Crystal Growth & Design* **2007**, *7*, 724–729.
(36) Murphy, D.; Rodríguez-CintrÓn, F.; Langevin, B.; Kelly, R. C.; Rodíguez-Hornedo, N. *Int. J. Pharm.* **2002**, *246*, 121–134.
(37) Nair, R.; Gonen, S.; Hoag, W. S. *Int. J. Pharm.* **2002**, *240*, 11–22.
(38) Li, Y.; Chow, P. S.; Reginald, B. H. T.; Black, S. N. *Org. Proc. Res. Dev.* **2008**, *12*, 264–270.

Table 1. **Design of experiments for the transformation process**

run	material	temperature (°C)	stirrer speed (RPM)	seeding
1	1.2 g CBZ[a]+350 mL H_2O	28	200	no
2	1.2 g CBZ[a]+350 mL H_2O	28	300	no
3	1.2 g CBZ[a]+350 mL H_2O	28	400	no
4	1.2 g CBZ[a]+350 mL H_2O	13	300	no
5	1.2 g CBZ[a]+350 mL H_2O	22	300	no
6	1.2 g CBZ[a]+350 mL H_2O	34	300	no
7	1.2 g CBZ[a]+350 mL H_2O	43	300	no
8	1.2 g CBZ[b]+350 mL H_2O	28	200	no
9	1.2 g CBZ[b]+350 mL H_2O	34	300	no
10	1.2 g CBZ[b]+350 mL (12 wt.% ethanol+88wt.%H_2O)	34	300	no
11	1.2 g CBZ[b]+350 mL H_2O	34	300	1 wt % seeds
12	10 g CBZ[a]+350 mL H_2O	28	200	no
13	repeat of experiment 12			

[a] Small size, raw materials (mean size 64 μm, by Malvern Mastersizer). [b] Large size, crystallized from the ethanol (mean size 222.09 μm, by Malvern Mastersizer).

that crystals of the form III are prismatic, whereas those of the CBZH are needlelike.

In situ FBRM and PVM measurements were performed during polymorphic transformation experiments. Preliminary experiments confirmed that the transformation from blocks of CBZ form III to thin needles of CBZH was accompanied by a large increase in Lasentec FBRM total counts. The FBRM probe measurement duration was set at 5 s, and the probe has a measurement range of 0.25−1000 μm. The PVM probe was operated with an image update rate of six images per minute.

A 500 mL jacketed glass vessel with an impeller (radial impeller with two lune blades and diameter 65 mm) was used for the experiments. To consider the influence of agitation rate, temperature, crystal size, and solvents on the polymorphic transformation, in situ polymorphic transformation experiments were performed at different temperatures (13−34 °C), agitation rates (200−400 rpm), crystal sizes, and solvents (water or ethanol−water mixture). The temperature was controlled from the jacket using a thermostatted bath. The stirring rate was controlled by the stirrer speed controller. The FBRM and PVM probes were inserted into the middle of the crystallizer at 15 mm under the surface. The crystals were sampled, and the polymorphous composition was analyzed by X-ray diffraction measurement. A series of trials were performed to examine the polymorphic transformation of CBZ (III to CBZH), and the trials are listed in Table 1.

The suspended solids were taken intermittently using a pipet, and then dropped on a slide. Offline digital image analysis was performed using a Panasonic Lumix DMC-FZ20 system operating Panasonic image analysis connected to a 3CCD color vision camera mounted on an Olympus BH2 optical microscope.

During the process of transformation, about 5−10 mL of slurry was transferred to a preheated, filter-equipped glass syringe (G2 grade) using a preheated transfer pipet. The filter liquor was analyzed by UV-spectrophotometry at 285 nm. The solids were measured by XRPD. The solubility (S_{CBZH}) was determined from the concentration of the slurry in water that was agitated for 24 h; the supersaturation values is C/S_{CBZH}, where C represents concentration.

X-ray powder diffraction of carbamazepine samples were obtained using the X-ray diffractometer (D/MAX 2500) at 40 kV, 200 mA and a scanning rate of 0.02°/min over the range 3−50°, using Cu Ka radiation of wavelength 1.5406 Å.The morphology of crystals (their habits and surface features) was examined with a scanning electron microscope (Philips 30 XL Holand) operating at 20 kV, 100 mA. The samples were mounted on a glass stub with double adhesive tape and coated under vaccum with gold in an argon atmosphere prior to observation.

Quantitative X-ray diffraction is an important technique for measuring the different amounts of polymorphs present in a system. The quantitative X-ray diffraction technique has been applied in many areas, such as the analysis of mine dust, quartz, heavy metal carbides, inorganic compounds, organic compounds, and pharmaceutical systems. The distinctly different PXRD patterns (Figure 2) of the two forms of CBZ have allowed us to quantitatively determine the phase transformation rate of the anhydrate form III into the dihydrate. By measuring the rate of disappearance or appearance of a unique peak, the kinetics of the transformation between two crystal forms can be determined. The ratio of two crystal forms in the slurry was evaluated on the basis of the relationship between the peak intensities (I) at the characteristic planes, as suggested by Zhu,[39] and then expressed as a percentage mass fraction of CBZ form III or CBZH, X, as described in eq 1,

$$X_A = I_{iA}/(I_{iA} + I_{jB}(I^o_A/I^o_B)) \quad (1)$$

where X_A is the mass fraction of CBZH and I_{iA} and I_{jB} are the intensity of diffraction peak of the ith and jth diffraction line of CBZH and CBZ form III, respectively. I^o_A and I^o_B represent the strongest diffraction peaks intensity of CBZH and CBZ form III, when $X_A = 1$ and $X_B = 1$, respectively. Quantitative analysis of polymorphic transformation was performed using XRD data, CBZH at 12.2°, CBZ form III at 15.7°, corresponding to the (020) reflection.

Result and Discussion

The influence of the stirring intensity on the polymorphic transformation of CBZ form III to CBZH at 28 °C is shown in Figure 4 with experiments 1, 2, and 3. The FBRM curves demonstrate that the particle counts increase quickly with the increase of agitation rates. The particle counts measured by FBRM are the most at 400 rpm, followed by 300 rpm, and 200 rpm gave the fewest particle counts. It is clearly shown that the mean size decreases when the stirring speed increases.

Figure 5 shows typical PVM photographs of CBZ form III transforming into CBZH at $t = 25$ min with the agitation rate of 200, 300, and 400 rpm, respectively. At an agitation rate of 200 rpm, after 25 min, the CBZH crystals grew to long and big, needlelike shapes, while the crystals are shorter and smaller at the stirring rates of 300 and 400 rpm. This fact coincides with the counts of particles measured by FBRM. At 400 rpm, the transformation slowed down after about 40 min. This is confirmed by the presence of the mostly needlelike morphology of CBZH crystals, and the particle counts change little at that

(39) Zhu, H. J.; Xu, J.; Varlashkin, P.; Long, S.; Kidd, C. *J. Pharm. Sci.* **2001**, *90*, 845–859.

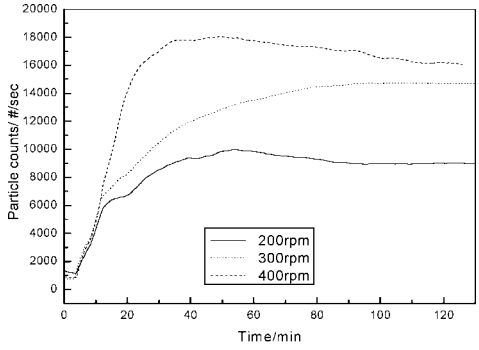

(a)Particle counts change with time

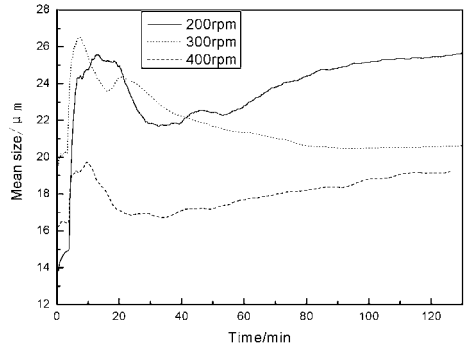

(b) Mean size change with time

Figure 4. **Curves of FBRM changes with time in experiments 1−3.**

time. At 200 and 300 rpm the transformations slowed down at $t = 70$ min and $t = 80$ min, respectively. This demonstrated that increasing the agitation rate can accelerate the transformation from form III to CBZH.

Figure 6 shows the curves of FBRM particle counts changes with time at different transformation temperatures of experiments 4, 5, 6 and 7. At the temperatures of 13 and 22 °C, the counts of particles measured by FBRM increased significantly after the addition of the crystals, then increased slowly, and finally the counts reached a constant value. This indicated that at a lower temperature the two processes, the dissolution of the metastable polymorph III of CBZ and the recrystallization (at $t_1 = 5$ min for 13 °C and at $t_2 = 10$ min for 22 °C) of the stable form CBZH, occur simultaneously. While at the temperature of 34 and 43 °C, the counts of particles increased first, then kept constant, and then increased until finally reaching equilibrium. This proves that the dissolution of the metastable polymorph III occurred first. Then the recrystallization (at $t_3 =$ 30 min for 34 °C, $t_4 = 54$ min for 43 °C) of the stable CBZH form occurred concomitantly with the dissolution of the metastable form III. Furthermore, it is notable that the counts of particles decreased with the increase of the temperature. The reason is that the solubility is higher at higher temperatures;[36] thus, a part of CBZ dissolved in the water and did not recrystallize. Also, at higher temperatures the thermodynamic driving force for the conversion to CBZH will be lower, which could account for the decrease in transformation rate.

Figure 7 is the chord length distribution of crystals at 13, 22, 34 and 43 °C at the stirrer speed of 300 rpm. Before 50 min, the nucleation and growth of CBZH are indicated by a steady rise in counts from FBRM chord length distribution, especially at lower chord length zone (0−18 μm). At 13 and

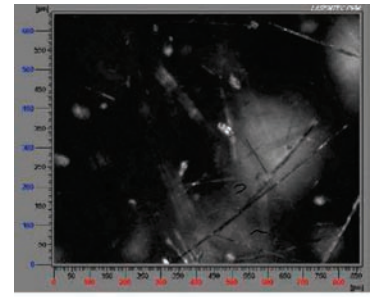

(a) 200rpm

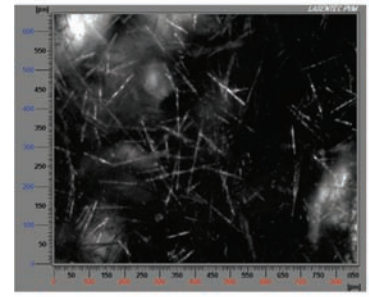

(b) 300rpm

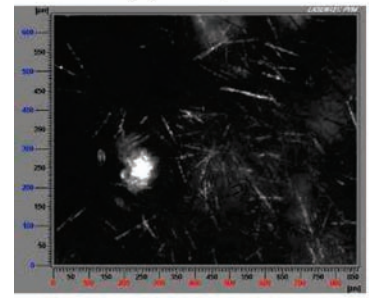

(c) 400rpm

Figure 5. **PVM images at 25 min with different agitation rates.**

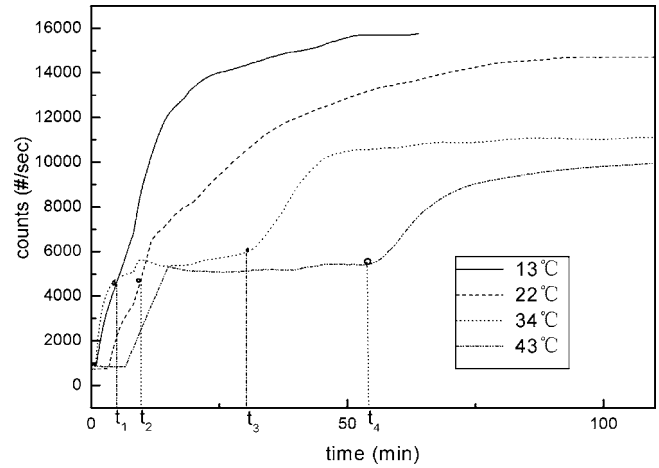

Figure 6. **Curves of FBRM particle counts changes with time of experiments 4−7.**

34 °C, after 50 min, little difference is found by FBRM chord length distribution and PVM images (not shown). With regard to Figure 7 at 43 °C, the higher temperature results in smaller dominant chord length. This may be because at higher temperatures, the solubility is higher; therefore; the yield is lower, and the crystals are smaller.

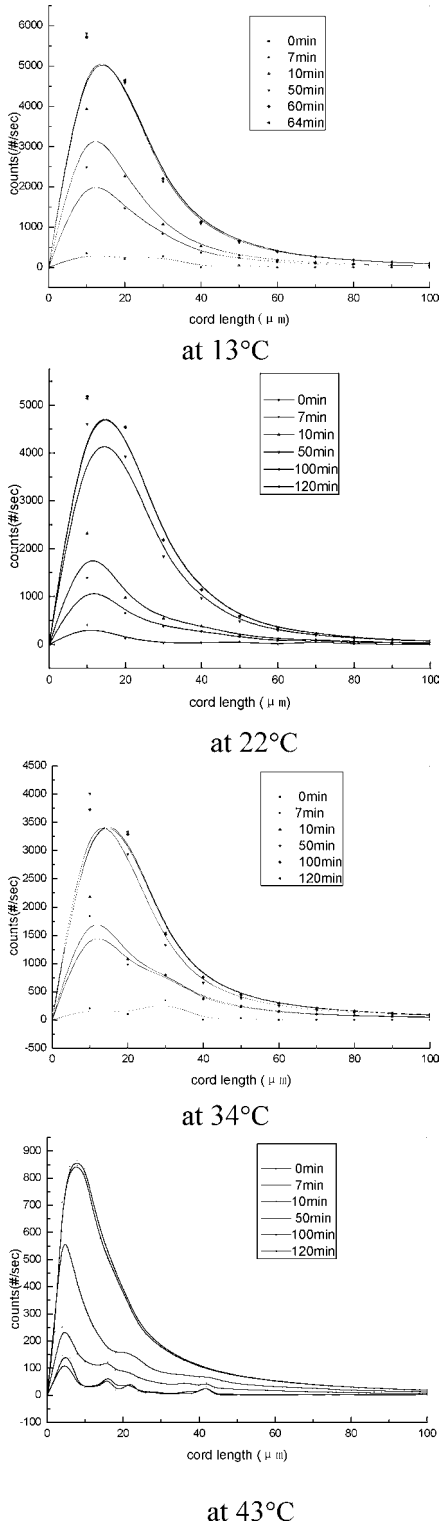

Figure 7. **Chord length distribution of particles at different temperatures and times (experiments 4−7).**

Figure 8 shows the curves of FBRM particle counts with different initial crystal sizes at the temperature of 28 °C with the agitation rate of 200 rpm. Small crystals shorted the anhydrous to dihydrate transformation times. From 5 to 20 min, needlelike crystals appeared and increased (Figure 9, experiment 1), corresponding to the steep increase of the particle counts by FBRM. After around 200 min, the transformation finished,

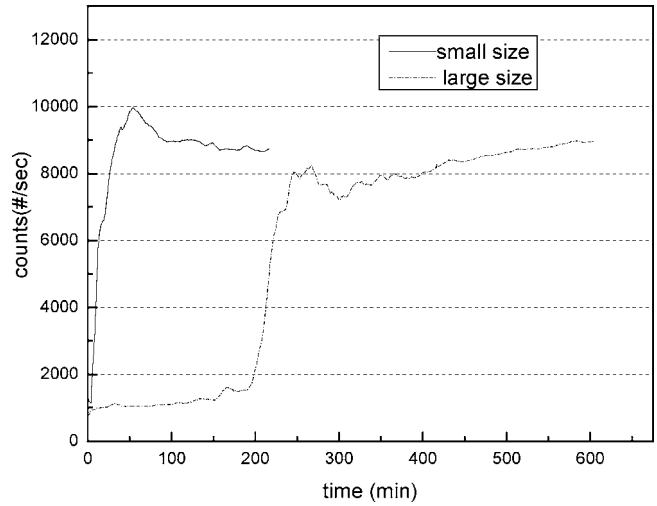

Figure 8. **Curves of FBRM particle counts change with time in experiments 1, 8.**

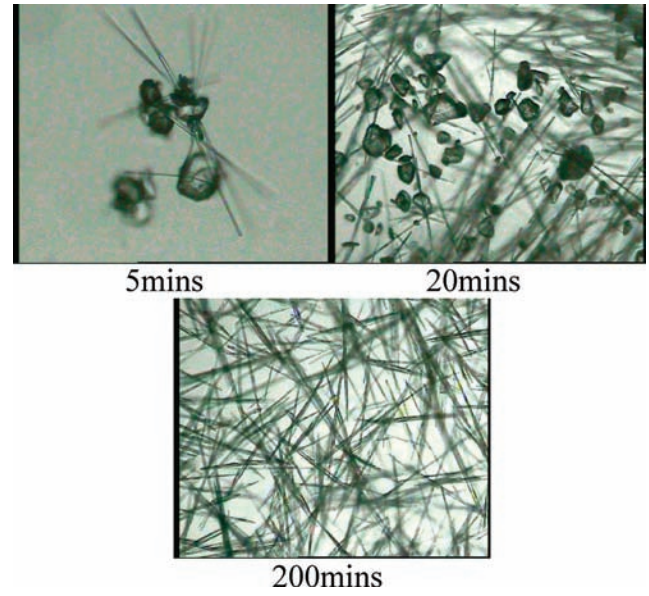

Figure 9. **Morphology changes with time.**

and only needlelike crystals existed, the particle counts reaching a nearly constant value.

The transformation time of the experiment with the larger initial crystal (form III) size is much slower than that of experiment with smaller size. The PVM images (not shown) showed that there were very few dihydrate crystals present and mostly the anhydrous solid phase remained suspended in solution at around 5 h. During the transformation, dihydrate crystals were observed as long needles in the bulk solution or on the surface of large and agglomerated crystals of CBZ form III.

The difference in the transformation rate between the above two experiments can be attributed to the difference in the nucleation rate or in the growth rate of CBZH. That is to say, when the crystal size is smaller, there are more crystals, and then more collisions happen; therefore, there is more nucleation. Or it because of more crystals, the surface area is greater, and so there is faster dissolution and more surface nucleation.

In order to estimate which is the rate-limiting step, crystallization of the dihydrate form or dissolution of the anhydrous

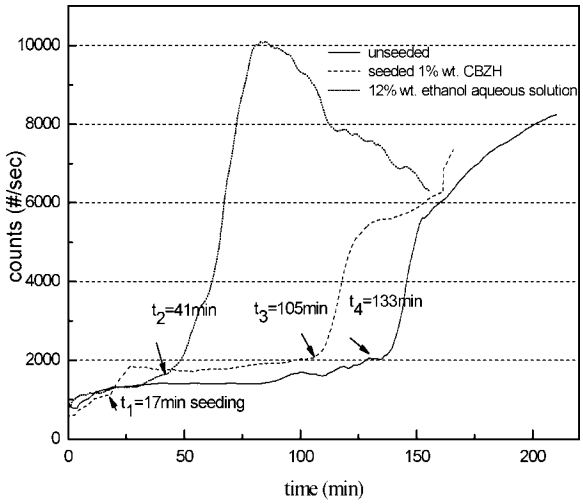

Figure 10. **Curves of FBRM particle counts changing with time in experiments 9−11.**

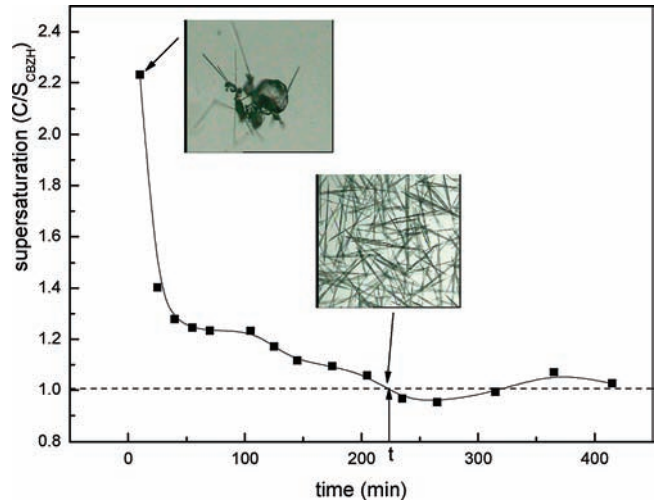

Figure 11. **Carbamazepine supersaturation−time profile of experiment 12.**

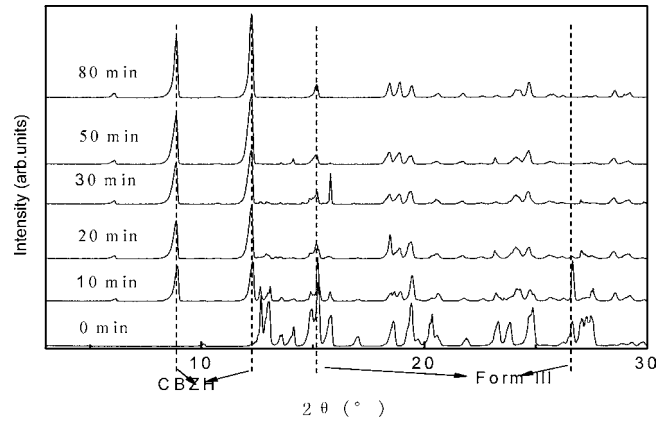

Figure 12. **XRD of CBZ sampled at different times in experiment 13.**

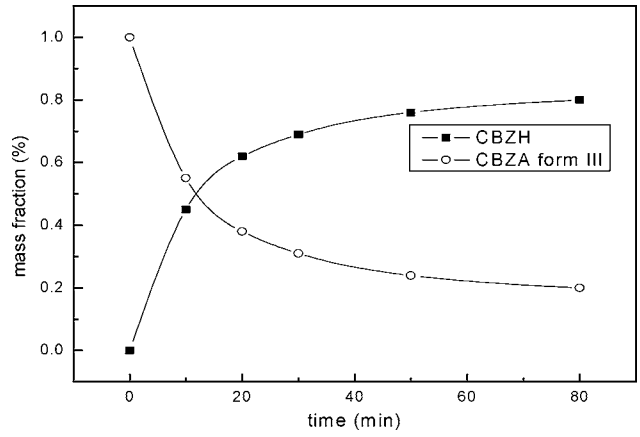

Figure 13. **Mass fraction changes of CBZH and CBZA with time in experiment 13.**

form, three more experiments 9, 10, and 11 were done. One is unseeded, one is seeded, and the other (unseeded) is the addition of ethanol into the solution. The temperature of the experiments is 34 °C, the agitation rate is 300 rpm, and the initial crystals are the larger size. Figure 10 consists of the curves of FBRM particle counts for the three experiments. For the seeded experiment, seeding resulted in a larger number of FBRM counts than observed in the unseeded experiment at the beginning at $t_1 = 17$ min. Then at $t_3 = 105$ min, more needlelike crystals (CBZH) appeared. In the unseeded experiment the FBRM counts began to increase significantly at the time of $t_4 = 133$ min. The transformation takes place slightly faster in the seeded experiment compared with that of the unseeded. This shows that nucleation may be the rate-limiting step during the process of the transformation.

Compared with the unseeded experiment, the addition of 12 wt % ethanol has a significant effect on the polymorphic transformation. At the time of t_2 (41 min), there is a steep increase of the FBRM counts, corresponding to the appearance of CBZH crystals. Addition of ethanol can increase the solubility because the solubility in pure ethanol is higher[40] than in water, and the solubility in water−ethanol is higher than in pure ethanol.[41] The driving force for dissolution increased, and also nucleation of CBZH was induced. It should be expected that the transformation rate is faster in solvents with high solubilities[42] because transformation rates will generally increase with solubility.

In order to measure the change of the solid composition, the experiment 12 was designed with high CBZ solid in the slurry. Figure 11 is the carbamazepine supersaturation−time profile. It can be seen that the decline in concentration approached the solubility of the stable phase (CBZH). Based on models developed by Cardew and Davey, [42] if dissolution is rate-limiting, supersaturation is 1.0 during the transformation. If growth is rate-limiting, supersaturation is 2.2 during the transformation (from reference 42, assuming that the solubility of CBZ is represented by a supersaturation of 2.2). Figures 11 and 13 suggest that supersaturation is constant at ~1.2 during most of the transformation (40−107 min and 40−80 min respectively for Figures 11 and 13). This suggests there maybe some other mechanism. This needs to be further investigated.

Experiment 13 is a repeat of the experiment 12. It is assumed that the transformation takes place in the same way in both experiments. Because of its outstanding ability, the X-ray diffraction technique has a high degree of accuracy and almost

(40) Liu, W. J.; Dang, L. P.; Black, S. N.; Wei, H. Y. *J. Chem. Eng. Data* **2008**, *53*, 2204–2206.
(41) Qu, H.; Marjatta, L. K.; Kallas, J. *Int. J. Pharm.* **2006**, *321*, 101–107.
(42) Cardew, P. T.; Davey, R. J. *Pro. R. Soc. Lond. A* **1985**, *398*, 415–428.

never fails to detect differences in crystal structures. Figure 12 is the XRD spectra at different time. In Figure 12 the typical change in the XRD pattern is shown. It can be seen that CBZ form III transforms to CBZH by the mixture of the III and CBZH forms (10 min, 20 min).The intensity of form III (specific peaks at 15.3°, 27.4°) decreased and of which CBZH (specific peaks at 8.8°, 12.2°) increased with the time. The transformation starts immediately (before 10min) and the transformation rate are quickly before 50minutes, and then slowed. This can be seen from the intensity of the peak at 27.4° of CBZ form III reflection dropped toward zero at t=50min. Monitoring the solid phase composition during the transformation indicates that the decrease in solution concentration (Figure 11) corresponds to an increase in the fraction of CBZH (Figure 13). From the optical micrographs in Figure 11, at the time of about $t = 220$ min, only needlelike crystals exist, it was determined the transformation finished.

Conclusions

The transformation process for the CBZ form III to CBZ dihydrate in aqueous slurries was studied using the in situ FBRM, PVM, and offline XRD. The operating factors were investigated. The results showed that increasing the agitation speed accelerated the transformation of CBZ from III to CBZH; a much longer time for CBZ form III to transform to CBZH was needed if the initial size of form III CBZ crystals was larger or the transformation temperature was higher. Addition of ethanol had a significant effect (shorted the transformation time) on the transformation. For the unseeded experiment, the transformation time was about 220 min, and seeding shortened the time by about 20 min. The transformation mechanism can be identified as a solution-mediated transformation from the experiments of an aqueous suspension of CBZ.

The FBRM can give the real-time information about particle size, and XRPD gives the precise crystal structure information. From PVM images, the real-time changes of the crystal shape were observed and showed that the crystal morphologies changed from a blocked shape to needlelike. Furthermore, it was shown that some CBZH crystals grew on the surface of form III crystals. Inline PVM was found more suitable to obtain insight into the transformation process. UV spectroscopy is cheap, easy to use, and can give good information. If in situ ATR-FTIR is available, it is also necessary to monitor concentration changes to gain a truer understanding during transformation.

Acknowledgment

We thank AstraZeneca UK Limited and National Nature and Science Foundation of China (NSFC, No. 20776098) for their financial assistances in this project.

Received for review October 27, 2008.

OP8002773